

# Vinculin and Rab5 Complex Is Required for Uptake of *Staphylococcus aureus* and Interleukin-6 Expression

Makoto Hagiwara<sup>1</sup>, Eitoyo Kokubu<sup>2</sup>, Shinsuke Sugiura<sup>1</sup>, Toshinori Komatsu<sup>1</sup>, Hiroyuki Tada<sup>1</sup>, Ryutaro Isoda<sup>1</sup>, Naomi Tanigawa<sup>1</sup>, Yoshiko Kato<sup>1</sup>, Naoyuki Ishida<sup>1</sup>, Kaoru Kobayashi<sup>1</sup>, Misako Nakashima<sup>1</sup>, Kazuyuki Ishihara<sup>2</sup>, Kenji Matsushita<sup>1\*</sup>

<sup>1</sup> Department of Oral Disease Research, National Center for Geriatrics and Gerontology, Obu, Aichi, Japan, <sup>2</sup> Department of Microbiology, Tokyo Dental College, Chiba, Japan

## Abstract

Vinculin, a 116-kDa membrane cytoskeletal protein, is an important molecule for cell adhesion; however, little is known about its other cellular functions. Here, we demonstrated that vinculin binds to Rab5 and is required for *Staphylococcus aureus* (*S. aureus*) uptake in cells. Vinculin directly bound to Rab5 and enhanced the activation of *S. aureus* uptake. Over-expression of active vinculin mutants enhanced *S. aureus* uptake, whereas over-expression of an inactive vinculin mutant decreased *S. aureus* uptake. Vinculin bound to Rab5 at the N-terminal region (1-258) of vinculin. Vinculin and Rab5 were involved in the *S. aureus*-induced phosphorylation of MAP kinases (p38, Erk, and JNK) and IL-6 expression. Finally, vinculin and Rab5 knockdown reduced infection of *S. aureus*, phosphorylation of MAPKs and IL-6 expression in murine lungs. Our results suggest that vinculin binds to Rab5 and that these two molecules cooperatively enhance bacterial infection and the inflammatory response.

**Citation:** Hagiwara M, Kokubu E, Sugiura S, Komatsu T, Tada H, et al. (2014) Vinculin and Rab5 Complex Is Required for Uptake of *Staphylococcus aureus* and Interleukin-6 Expression. PLoS ONE 9(1): e87373. doi:10.1371/journal.pone.0087373

**Editor:** David M. Ojcius, University of California Merced, United States of America

**Received:** November 5, 2013; **Accepted:** December 24, 2013; **Published:** January 23, 2014

**Copyright:** © 2014 Hagiwara et al. This is an open-access article distributed under the terms of the Creative Commons Attribution License, which permits unrestricted use, distribution, and reproduction in any medium, provided the original author and source are credited.

**Funding:** This work was supported by a Grant-in-Aid for Scientific Research B (to K.M.). The funders had no role in study design, data collection and analysis, decision to publish, or preparation of the manuscript.

**Competing Interests:** The authors have declared that no competing interests exist.

\* E-mail: kmatsu30@ncgg.go.jp

## Introduction

Rab small GTPases are conserved membrane trafficking proteins in all eukaryotes, and they mediate various steps in membrane trafficking, including vesicle budding, vesicle movement, vesicle docking to specific membranes, and vesicle fusion [1]. Rab cycling between the GDP-bound (inactive) form and the GTP-bound (active) form is regulated by guanine nucleotide exchange factors (GEF), GTPase-activating proteins (GAPs), and GDP dissociation inhibitors [2]. This strict control is critical for the correct activation of Rab in time and space. More than 60 Rabs have been identified so far. Each Rab is localized to a specific membrane and controls a specific transport step [1,3]. For example, Rab5 is localized to early endosomes and the plasma membrane, and it is essential for early stages of endocytosis and for fusion of the early endosome [4,5]. Rab5 has been shown to be involved in the internalization of many extracellular materials such as nutrients [6], growth factors [7,8,9], viruses [10,11,12,13] and bacteria [14,15,16,17]. A large number of Rab5-interacting proteins including EEA1 [18,19], Rabaptin-5 [20,21,22], phosphatidylinositol 3-kinases [23,24], Rabankyrin-5 [25,26], Vps3 [27], Vps8 [27], POT1 [28] and caveolin [29,30] have been identified. Identification of Rab5-interacting proteins has provided insights into the molecular mechanism of endocytosis. We recently identified plastins as Rab5-binding proteins and shows that these proteins are not only actin-binding proteins but also endocytosis regulators [31].

Vinculin is a 116-kDa cytoskeletal protein that is involved in the linkage of integrin adhesion molecules to the actin cytoskeleton [32]. Vinculin interacts with many proteins including talin [33,34,35], alpha-actinin [36], F-actin [37,38], ARP2/3 [39], catenin [40,41,42,43], Paxillin [44], Hic-5 [44], VASP [45] and vinexin [46,47,48]. Structurally, vinculin is divided into three main domains: an N-terminal head, a flexible proline-rich hinge (neck) region, and a C-terminal tail domain [49]. The protein's activity is regulated by conformational reorganization of these domains. Intramolecular associations between the head and tail domains constrain vinculin in an inactive conformation, causing it to be located within the cytoplasm [49]. The structure of vinculin can change to an open state (active conformation) that facilitates its localization to the plasma membrane [35,50]. Many researchers have used various vinculin mutants to study the function of vinculin. Vinculin 8/19 (vin8/19) and vinculin T12 (vinT12) mutants interfere with the head-tail interaction characterizing constitutive activation [51]. The vinculin A50I (vinA50I) mutant inhibits the head/tail dissociation of vinculin [52] and increases the vinculin turnover rate in focal adhesions [53]. Vinculin can bind to phosphatidylinositol 4,5-bisphosphate (PIP2) and has two lipid-binding sites: CT and H3 [50,54]. The vinculin CT (vinCT) mutant was mutated in the CT lipid-binding site, the vinculin H3 (vinH3) mutant was mutated in the H3 lipid-binding site, and the vinculin LD (vinLD) mutant was mutated in both the CT and H3 lipid-binding sites. These mutants were deficient in PIP2. In addition, the vinculin D1 domain (residues 1-258) bound to talin and alpha-actinin by using vinculin deletion mutants [32]. A previous

study showed by using collagen-coated beads that vinculin may be involved in cellular [55]. However, molecular mechanism of endocytosis by vinculin is still not clear.

Cellular responses to many external stimuli involve the activation of several types of MAPK signaling pathways. MAPKs are a family of serine/threonine kinases that comprise three major subgroups: ERKs, p38, and JNKs [56,57]. MAPKs can be localized to early endosomes by various external stimuli via endocytosis, thereby transmitting signals to downstream [58,59,60,61]. These proteins regulate the expression of many inflammatory cytokines including IL-6 [56,57].

*Staphylococcus aureus* (*S. aureus*), a gram-positive pathogen, has long been recognized as one of the most important bacteria that cause various diseases such as bloodstream infections, bone and joint infections, and pneumonia. *In vitro* studies have shown that *S. aureus* is internalized [62] and survives inside non-phagocytic cells [63,64,65]. Internalized *S. aureus* is able to evade or delay elimination by the host's immune system and avoid extracellular antibiotics [66]. However, the invasive mechanism and the effect of *S. aureus* on host cells remain a mystery. In this study, we showed the role of vinculin–Rab5 interaction in the uptake of *S. aureus* into non-phagocytic cells and the relationship between these proteins and phosphorylation of MAPK and IL-6.

## Materials and Methods

### Ethics statement

This study was carried out in strict accordance with the recommendations in the Guide for the Care and Use of Laboratory Animals of the National Institutes of Health. The protocol was approved by the Committee on the Ethics of Animal Experiments of Tokyo Dental College.

### Cell culture

Cos-7 cells (RIKEN BIORESOURCE CENTER) were cultured in DMEM (Wako) supplemented with 10% FBS, 1% penicillin, and 1% streptomycin. HeLa cells (RIKEN BIORESOURCE CENTER) were cultured in Advanced MEM (Sigma) supplemented with 5% FBS, 1% penicillin, and 1% streptomycin.

### Antibodies

Antibodies were obtained from the following sources: anti-mouse HA and anti-rabbit HA (Sigma); anti-rabbit IgG-Alexa 555 and anti-rabbit IgG-Alexa 633 (Invitrogen); anti-rabbit Rab5, anti-mouse GFP, and anti-rabbit GFP (Novus); anti-mouse p38, anti-mouse JNK, and anti-mouse Erk (BD bioscience); anti-rabbit phospho-p38, anti-rabbit phospho-JNK, and anti-rabbit phospho-Erk (Cell Signaling Technology); anti-mouse vinculin, anti-IL-6, and anti-rabbit *S. aureus* (Abcam); anti-mouse IgG-HRP and anti-rabbit IgG-HRP (IBL); anti-GST HRP conjugate (Amersham Bioscience); anti-mouse GAPDH (MBL); and anti-mouse His (Sino Biological).

### Vector constructs

GFP-Rab5 (WT; wild type), GFP-Rab5S34N, and GFP-Rab5Q79L in pcDNA3 and GST-Rab5Q79L and GST-Rab5S34N in pGEX-2T constructs were kindly provided by Dr. Y. Yamamoto (Tokyo University of Agriculture, Tokyo, Japan). For the expression of HA-fused proteins, Rab5Q79L, Rab5 (WT), and Rab5S34N DNAs were amplified by PCR and cloned into pCMV-HA. The GST-R5BD vector was kindly donated by Dr. G. Li (University of Oklahoma Health Science Center, Oklahoma City, USA). GFP-vinculin (GFP-vinWT), GFP-vinculin8/19

(GFP-vin8/19), and GFP-vinculinT12 (GFP-vinT12) vectors were kindly provided by Dr. S. W. Craig (The Johns Hopkins School of Medicine, Baltimore, USA). The pTag RFP-vinculin vector was obtained from Evrogen Inc. vin1-258, vin1-880, vin258-880, vin881-1066, and vin1-1066 (vinWT) were amplified by PCR and cloned into the vector pet30a or pcDNA3-GFP. GFP-vinculinA50I (GFP-vinA50I) was constructed by mutating wild-type vinculin using a QuikChange Site-Directed Mutagenesis Kit (STRATAGEN) according to the manufacturer's instructions.

### Expression in *Escherichia coli* and purification of proteins

GST-Rab5Q79L, GST-Rab5S34N, GST, and GST-R5BD were expressed in BL21-Codon Plus and purified as described previously [29,67,68,69]. His-vin1-258, His-1-880, His258-880, His881-1066, and His-vin1-1066 (full length) were expressed in BL21-Codon Plus and purified with His Mag sepharose Ni (GE Healthcare) according to the manufacturer's instructions.

### Immunoprecipitation

To analyze the binding of vinculin and Rab5, cells were transfected with the indicated plasmids and lysed for 30 min at 4°C with a buffer (10 mM Tris, pH 7.6, 150 mM NaCl, 5 mM MgCl<sub>2</sub>, 1% NP-40, 0.5 µg/mL leupeptin, 2 µg/mL aprotinin, and 10 µg/mL PMSF). The clarified lysates were incubated with antibodies for 2 h at 4°C. The immune complexes were precipitated with protein A–Sepharose (Millipore) for 2 h at 4°C and then washed extensively with lysis buffer. The beads were resuspended in SDS sample buffer and assayed by western blotting.

### GST-Rab5 pull-down assays

Five µg GST-Rab5Q79L or GST-Rab5S34N was added to 40 µL of glutathione–Sepharose resin and incubated for 1 h at 4°C. The beads were washed with a wash buffer (20 mM HEPES, 100 mM NaCl, 5 mM MgCl<sub>2</sub>, and 1 mM dithiothreitol, pH 7.6), incubated with the cell lysate or purified His-vinculin for 60 min at 4°C, washed three times with the wash buffer, resuspended in an SDS sample buffer (62.5 mM Tris pH 6.8, 2% SDS, 10% glycerol and 100 mM 2-mercaptoethanol, 0.005% BPP), and analyzed by western blotting.

### Uptake assay

To measure the uptake of transferrin, albumin, and Lucifer yellow, cells were pre-incubated with serum-free DMEM without phenol red for 1 h at 37°C in 24-well plates and then incubated with 50 µg/mL transferrin Alexa Fluor 555 (Invitrogen), 50 µg/mL albumin Alexa Fluor 555 (Invitrogen), or 1 mg/mL Lucifer yellow lithium salt (Sigma) diluted with serum-free DMEM without phenol red for 2 h at 37°C or 4°C to measure the background level of uptake (negative control). After incubation, the cells were collected with ice-cold PBS, washed eight times with ice-cold PBS, lysed with PBS containing 1% Triton X-100, and centrifuged at 10,000×g for 20 min at 4°C. The signal intensity of the supernatant was measured using SpectraMax M3 (Molecular Devices).

To measure FM4-64 uptake, cells were pre-incubated with serum-free DMEM without phenol red for 1 h at 37°C in 96-well plates. Subsequently, 100 µg/mL FM4-64 (Invitrogen) diluted with serum-free DMEM without phenol red was added to the cells. Immediately, fluorescence from extracellular FM4-64 was analyzed using SpectraMax M3 to measure the background level of uptake. The cells were then incubated for 2 h at 37°C, and

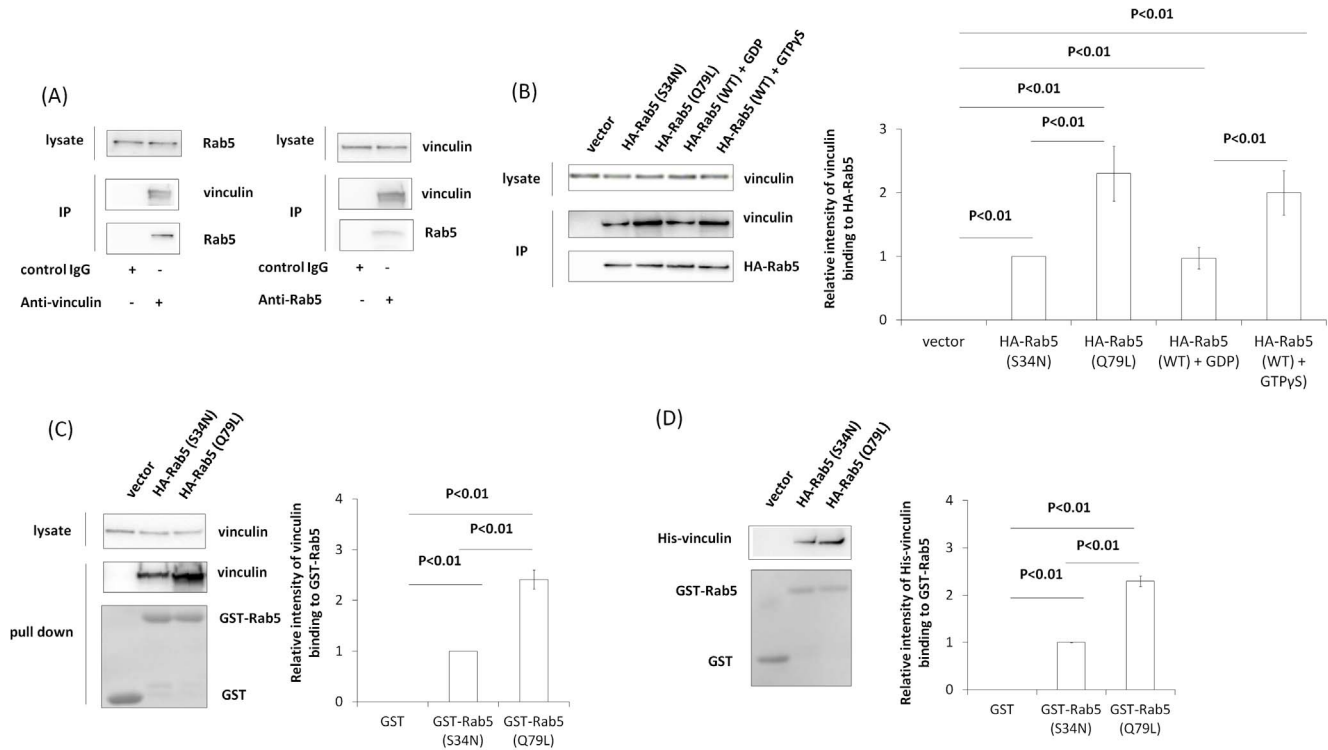


**Figure 1. Direct binding of vinculin and Rab5.** (A) Endogenous vinculin and Rab5 were immunoprecipitated from Cos-7 lysates with anti-Rab5 or anti-vinculin antibodies. Vinculin and Rab5 were assayed by western blotting using specific antibodies to vinculin and Rab5. (B) HA-Rab5 (S34N), HA-Rab5 (Q79L) and HA-Rab5 (WT) were transiently expressed in Cos-7 cells and subjected to immunoprecipitation with anti-HA antibody. Note that immunoprecipitation of HA-Rab5 (WT) was carried out with GTP $\gamma$ S and GDP. Proteins were assayed by western blotting. The graph shows mean  $\pm$  S.E. values of three independent experiments (C) A pull-down assay from a Cos-7 lysate was performed using GST, GST-Rab5 (S34N), and GST-Rab5 (Q79L). Vinculin bound to the beads was assayed by western blotting, and GST, GST-Rab5 (S34N), and GST-Rab5 (Q79L) on a PVDF membrane were stained with Ponceau S. The graph shows mean  $\pm$  S.E. values of three independent experiments (D) GST, GST-Rab5 (S34N), and GST-Rab5 (Q79L) were incubated with purified His-vinculin, and a pull-down assay was performed using glutathione beads. His-vinculin bound to the beads was assayed by western blotting, and GST, GST-Rab5 (S34N), and GST-Rab5 (Q79L) on a PVDF membrane were stained with Ponceau S. The graph shows mean  $\pm$  S.E. values of three independent experiments.  
doi:10.1371/journal.pone.0087373.g001

signal intensity was measured using SpectraMax M3 (Molecular Devices).

To measure *S. aureus* uptake, the cells were pre-incubated with serum-free DMEM without phenol red for 1 h at 37°C in 96-well plates. Subsequently, 1 mg/mL pHrodo red-labeled *S. aureus* BioParticles (Invitrogen) diluted with serum-free DMEM without phenol red was added to the cells. The cells were incubated for 2 h at 37°C, and signal intensity was measured using SpectraMax M3 (Molecular Devices).

### Immunostaining

Cells were fixed with 4% formaldehyde in PBS for 10 min and washed with PBS. Nonspecific binding of antibodies was blocked by incubation with 5% sheep serum in TBS-T for 60 min, followed by washing with TBS-T. The cells were incubated with a primary antibody in TBS-T for 60 min and washed with PBS. Bound primary antibodies were visualized with a secondary antibody in buffer A (10 mM Tris, pH 7.6, 300 mM NaCl, and 0.5% Tween 20). After extensive washing with buffer A, cells were mounted on slide glasses. The cells were observed using a confocal fluorescence microscope (Carl Zeiss Co., Ltd).

### Over-expression of proteins in cultured cells

Each DNA plasmid was transfected with Lipofectamine 2000 (Invitrogen) according to the manufacturer's instructions.

### Knockdown in cultured cells

Rab5 siRNA (catalog no. RAB5A-HSS108976), vinculin siRNA (catalog no. VCL-HSS111259), Stealth RNAi Negative Control Low GC Duplex, and Stealth RNAi Negative Control Medium GC Duplex were obtained from Invitrogen. These siRNAs were transfected with Lipofectamine 2000 (Invitrogen) according to the manufacturer's instructions.

### GST-R5BD pull-down assay

One hundred  $\mu$ g/mL *S. aureus* was added to the medium of cells transfected with GFP-Rab5 and incubated for indicated times at 37°C. The GST-R5BD pull-down assay was then performed as described previously [67,70,71] to measure the Rab5-GTP level. In brief, the cells were washed two times with PBS and lysed for 5 min in 1 mL lysis buffer (25 mM HEPES, pH 7.4, 100 mM NaCl, 5 mM MgCl<sub>2</sub>, 0.1% NP-40, 2% glycerol, 1 mM DTT, 0.5  $\mu$ g/mL leupeptin, 2  $\mu$ g/mL aprotinin, and 10  $\mu$ g/mL PMSF). Lysis extracts were clarified by centrifugation at 10,000 $\times$ g for 5 min at 4°C, and supernatants were incubated with 20  $\mu$ L of GST-R5BD bound to glutathione-Sepharose 4B beads for 20 min at 4°C with slow stirring. The beads were subsequently washed with lysis buffer, re-suspended in SDS sample buffer, and assayed by western blotting.

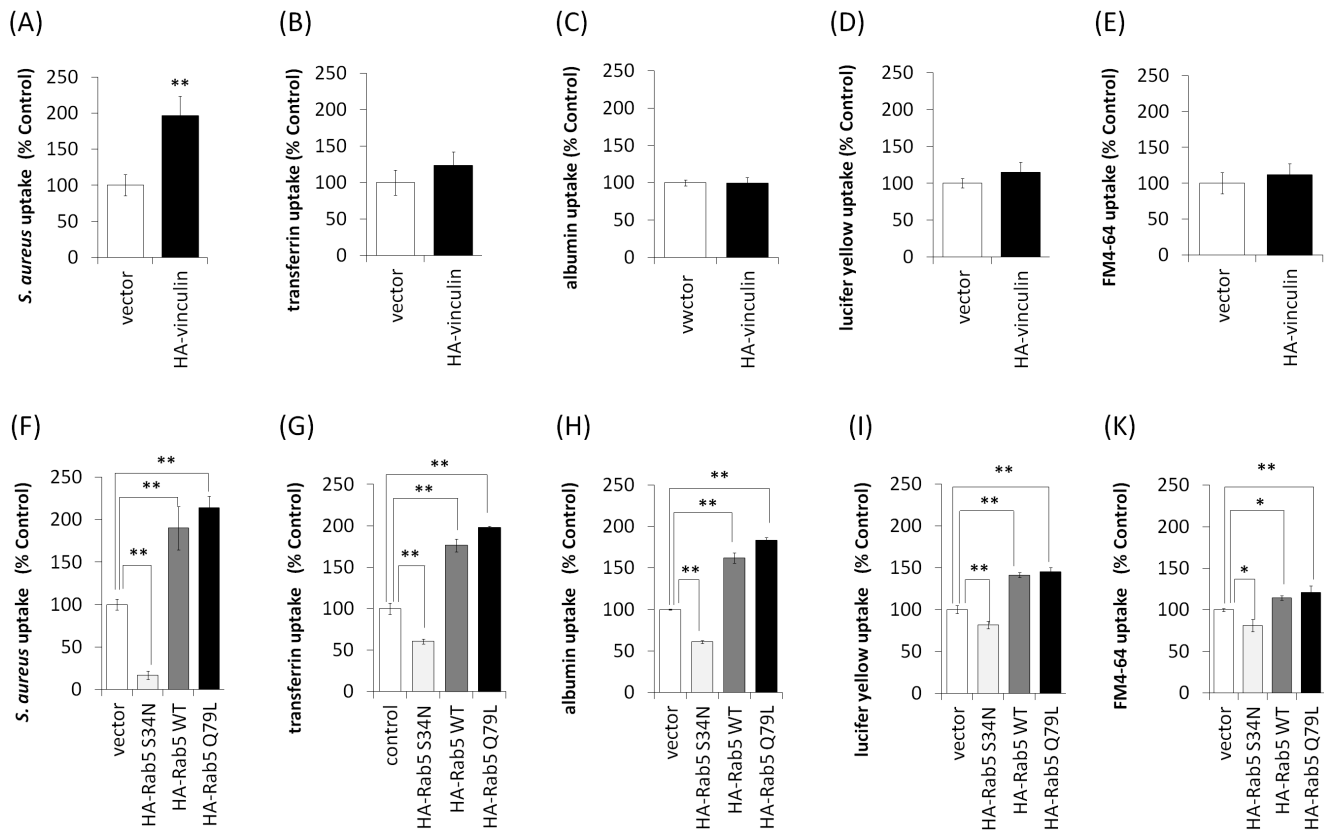


**Figure 2. Effect of vinculin and Rab5 expression on cellular uptake.** (A–E) HA-vinculin-expressing Cos-7 cells were incubated with various markers of uptake at 37°C for 2 h. Uptake of pHrodo red-labeled *S. aureus* BioParticles increased in HA-vinculin-expressing cells, but the uptake of transferrin Alexa 555, albumin Alexa 555, Lucifer yellow and FM 4-64 did not increase. Error bar:  $n = 3-6 \pm SE$ ,  $**p < 0.01$ . (F–H) HA-Rab5 (S34N)-, HA-Rab5 (WT)-, and HA-Rab5 (Q79L)-expressing Cos-7 cells were incubated with various uptake indicators at 37°C for 2 h. Uptake of pHrodo red-labeled *S. aureus*, transferrin Alexa 555, albumin Alexa 555, Lucifer yellow, and FM 4-64 increased in HA-Rab5 (WT)- and HA-Rab5 (Q79L)-expressing cells, whereas uptake of each of the indicators was decreased in HA-Rab5 (S34N)-expressing cells. Error bar:  $n = 3-6 \pm SE$ ,  $*p < 0.05$ ,  $**p < 0.01$ . doi:10.1371/journal.pone.0087373.g002

### Effect of *S. aureus* on vinculin–Rab5 binding

Cells were pre-incubated with DMEM for 1 h at 37°C in 6-well plates. After pre-incubation, 100  $\mu\text{g}/\text{mL}$  *S. aureus* (Invitrogen) was added to tissue culture cells, followed by incubation for the indicated time. The cells were then washed with PBS and lysed with lysis buffer (25 mM HEPES, pH 7.4, 100 mM NaCl, 5 mM  $\text{MgCl}_2$ , 0.1% NP-40, 2% glycerol, and 1 mM DTT) containing protease inhibitors. The lysates were subjected to immunoprecipitation or the GST-R5BD pull-down assay as described earlier.

### Bacterial strain

*S. aureus* 209P was preserved at Tokyo Dental College. *S. aureus* 209P was grown in trypticase soy broth medium.

### Animals

Specific pathogen-free BALB/c female mice (age, 10 weeks) were obtained from Sankyo Labo Service Corporation, Inc., Tokyo, Japan. All mice were given sterile food and water *ad libitum* under conventional conditions in the animal care facility of Tokyo Dental College. This study was carried out in accordance with “Guidelines for the Treatment of Experimental Animals in Tokyo Dental College” [72].

### Knockdown *in vivo*

*In vivo* grade siRNA for Rab5 (catalog no. RAB5A-MSS212350), siRNA for vinculin (catalog no. VCL-MSS241137), Stealth RNAi Negative Control Low GC Duplex, and Stealth RNAi Negative Control Medium GC Duplex were obtained from Invitrogen. Two hundred fifty  $\mu\text{L}$  of 3 mg/mL siRNA was diluted to 1.5 mg/mL with 250  $\mu\text{L}$  complexation buffer accessory for invivolectamine (Invitrogen). Five hundred  $\mu\text{L}$  of the diluted siRNA solution was mixed with 500  $\mu\text{L}$  invivolectamine, and incubated for 30 min at 50°C. Forty  $\mu\text{L}$  of the mixture was injected into murine lungs via direct transtracheal instillation (30  $\mu\text{g}$  siRNA per mouse). Note that Rab5 and vinculin knockdown continues for more than week (data not shown).

### Infection of *S. aureus* in murine lungs

Ten-week-old BALB/c female mice were infected with bacteria via direct transtracheal instillation with minor modifications [72]. The mice were anesthetized by injection of thiopental sodium (Ravonal, Tanabe-Mitsubishi, Osaka, Japan), and a surgical incision was made in the neck to expose the trachea. Approximately  $2 \times 10^7$  cfu of *S. aureus* 209P diluted in 50  $\mu\text{L}$  PBS was instilled into the trachea using a 30-gauge needle. The incision was closed with a suture, and the mice were monitored over the next 3 days. The mice were sacrificed, and bronchoalveolar lavage (BAL) was performed three times with 1 mL sterile PBS. The lung was then removed and homogenized in sterile PBS, and diluted

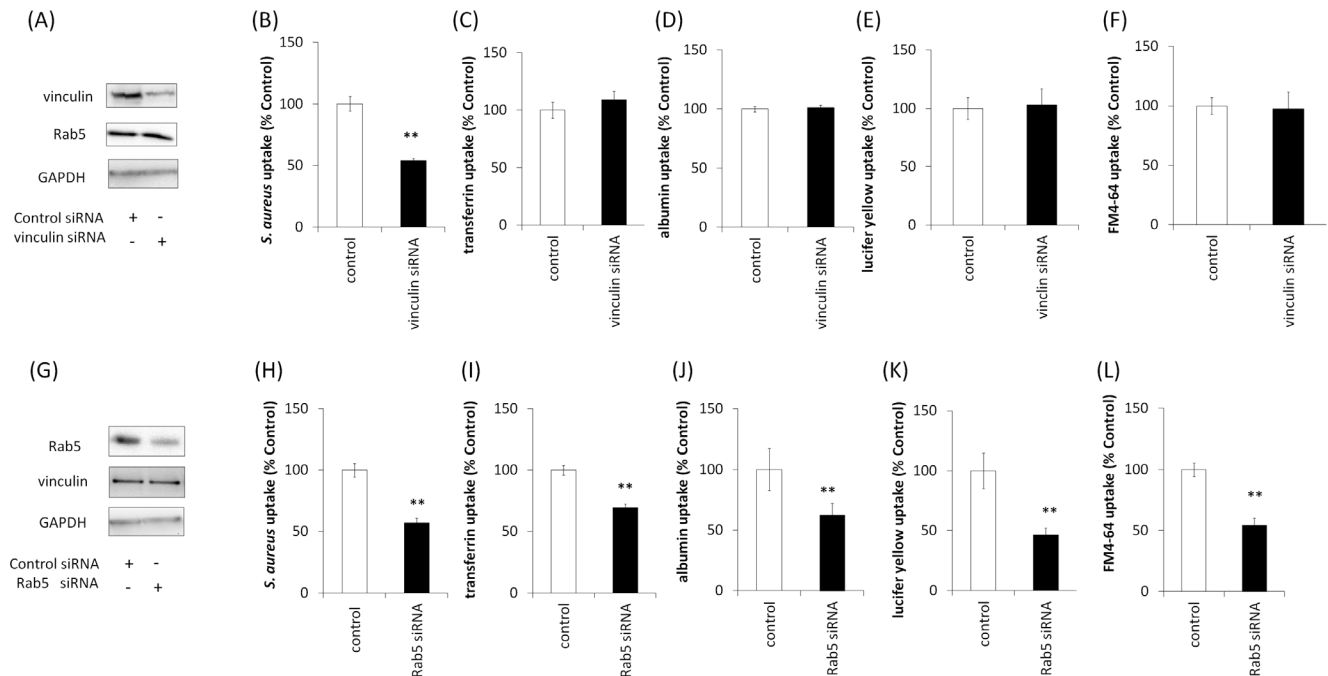


**Figure 3. Effects of vinculin and Rab5 knockdown on cellular uptake.** (A) siRNAs for vinculin were transfected into HeLa cells, and cell lysates were assayed by western blotting using anti-vinculin, anti-Rab5, and anti-GAPDH antibodies (internal control). (B–F) Various uptake indicators were added to the media of vinculin knockdown cells and incubated at 37°C for 2 h. Uptake of pHrodo red-labeled *S. aureus* decreased, but that of transferrin Alexa 555, albumin Alexa 555, Lucifer yellow, and FM 4-64 did not decrease. Error bar:  $n = 3-6 \pm SE$ , \*\* $p < 0.01$ . (G) siRNAs for Rab5 were transfected into HeLa cells and cell lysates were assayed by western blotting with anti-Rab5, anti-vinculin, and anti-GAPDH antibodies. (H–L) HeLa cells transfected with Rab5 siRNA. Various uptake indicators were added to the media of Rab5 knockdown cells and incubated at 37°C for 2 h. Uptake of pHrodo red-labeled *S. aureus*, transferrin Alexa 555, albumin Alexa 555, Lucifer yellow, and FM 4-64 was decreased. Error bar:  $n = 3-6 \pm SE$ , \*\* $p < 0.01$ .

doi:10.1371/journal.pone.0087373.g003

homogenate was plated onto trypticase soy agar plates. The plates were cultured at 37°C, after which colonies were counted as cfu.

## Statistics

Data were compiled and analyzed using Ezanova software. Statistical significance was defined as  $p < 0.05$ .

## Results

### Vinculin binding with Rab5

To investigate whether vinculin can bind to Rab5, we performed immunoprecipitation using Cos-7 lysates. Endogenous vinculin and Rab5 were coimmunoprecipitated with both anti-vinculin and anti-Rab5 for immunoprecipitation (Fig. 1A). We then investigated whether vinculin interacts with inactive Rab5 and/or active Rab5. HA-Rab5 (Q79L) (activated mutant), HA-Rab5 (S34N) (inactivated mutant) and HA-Rab5 (WT) were overexpressed in Cos-7 cells and immunoprecipitated using anti-HA antibody. Immunoprecipitation showed that vinculin bound to both HA-Rab5 (Q79L) and HA-Rab5 (S34N), but bound more strongly to HA-Rab5 (Q79L) than to HA-Rab5 (S34N) (Fig. 1B). It is also showed that vinculin bound to both HA-Rab5 (WT)-GTP $\gamma$ S and HA-Rab5 (WT)-GDP, but bound more strongly to HA-Rab5 (WT)-GTP $\gamma$ S than to HA-Rab5 (WT)-GDP (Fig. 1B). We next tested vinculin–Rab5 interaction by the GST pull-down assay. GST pull-down assays using Cos-7 cell lysates also showed that vinculin bound to both GST-Rab5 (Q79L) and GST-Rab5 (S34N) but bound more strongly to GST-Rab5 (Q79L) than to GST-Rab5 (S34N) (Fig. 1C). Purified His-vinculin also bound

strongly to GST-Rab5 (Q79L) (Fig. 1D). Together, these results indicate that vinculin can interact directly with Rab5 *in vitro*.

### Effect of vinculin and Rab5 on uptake

We hypothesized that vinculin plays a role in cellular uptake, given that Rab5 is important for endocytosis. We performed uptake assays using various markers. HA-vinculin over-expression increased the uptake of *S. aureus* (Fig. 2A) but not that of transferrin, albumin, Lucifer yellow, or FM4-64 in Cos-7 cells (Fig. 2B–E). In contrast, HA-Rab5Q79L and HA-Rab5 (WT) over-expression increased the uptake of *S. aureus*, transferrin, albumin, Lucifer yellow, and FM4-64, whereas HA-Rab5S34N over-expression decreased their uptake (Fig. 2F–K). To further investigate the effect of vinculin and Rab5 knockdown on uptake, we performed knockdown with specific siRNAs. As shown in Fig. 3A, introducing vinculin siRNA into HeLa cells inhibited vinculin expression. Vinculin knockdown decreased the uptake of *S. aureus* in HeLa cells (Fig. 3B) but not that of transferrin, albumin, Lucifer yellow, or FM4-64 (Fig. 3C–F). As shown in Fig. 3G, introducing Rab5 siRNA into HeLa cells inhibited Rab5 expression. With Rab5 knockdown, uptake of *S. aureus*, transferrin, albumin, Lucifer yellow, and FM4-64 was inhibited in HeLa cells (Fig. 3H–L). These results suggested that Rab5 is involved in the uptake of various markers, whereas vinculin is involved in only *S. aureus* uptake.

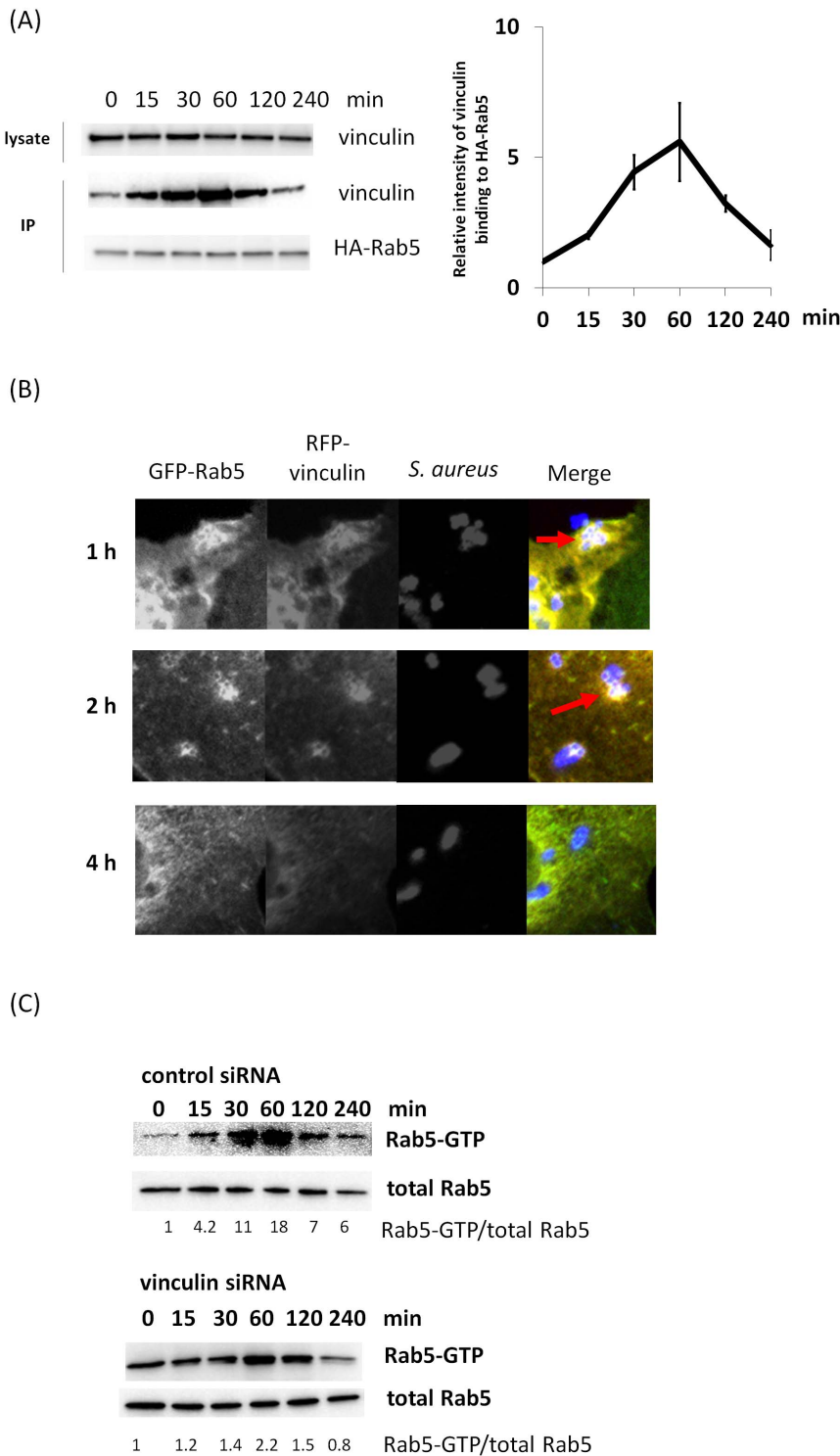


**Figure 4. Effects of *S. aureus* on vinculin-Rab5 binding and Rab5-GTP.** (A) *S. aureus* was added to the medium of HA-Rab5 (WT)-transfected Cos-7 cells and incubated with *S. aureus* for the indicated time at 37°C. The cells were lysed and subjected to immunoprecipitation with anti-HA antibody. Immunocomplexes were assayed by western blotting with anti-HA and anti-vinculin antibodies. Proteins levels were quantified using ImageJ in three independent experiments. (B) *S. aureus* was added to the medium of Cos-7 cells expressing GFP-Rab5 (WT) and RFP-vinculin (WT) and incubated for the indicated time at 37°C. The cells were fixed and immunostained with *S. aureus* antibodies. (C) HeLa cells were transfected with GFP-Rab5 (WT) and vinculin siRNA or control siRNA. *S. aureus* was added to the medium of transfected cell and incubated for the indicated time at 37°C. The cells were lysed and subjected to a GST-R5BD pull-down assay. GST-R5BD-bound beads and lysates were assayed by western blotting with anti-GFP antibody. Rab5-GTP levels were normalized to total GFP-Rab5 levels and quantified using ImageJ. doi:10.1371/journal.pone.0087373.g004

## Effects of *S. aureus* on vinculin-Rab5 binding and Rab5-GTP

Since both vinculin and Rab5 were shown to be involved in *S. aureus* uptake (Fig 2A and F and Fig. 3B and H), we next investigated the effect of *S. aureus* on vinculin-Rab5 interaction. *S. aureus* was added to HA-Rab5 (WT)-expressing Cos-7 cells, and the cell lysate was immunoprecipitated with anti-HA antibody. As shown in Fig. 4A, vinculin-Rab5 interaction increased up to 60 min following the addition of *S. aureus*. We further examined the effect of *S. aureus* on vinculin-Rab5 interaction with confocal fluorescence microscopy. *S. aureus* was added to GFP-Rab5 (WT) and RFP-vinculin-expressing Cos-7 cells, and the cells were immunostained with anti-*S. aureus*. Confocal fluorescence microscopic analysis showed that RFP-vinculin colocalized with GFP-Rab5 on *S. aureus* positive endosomes in Cos-7 cells at 1 and 2 h (Fig. 4B), whereas RFP-vinculin did not colocalize with GFP-Rab5 at 4 h. These findings indicate that *S. aureus* is involved in the vinculin-Rab5 interaction in the early stage of endocytosis.

We then performed a GST-R5BD pull-down assay [67] to investigate Rab5 activation in cultured cells. To investigate the effect of vinculin on Rab5 activation in *S. aureus* uptake, *S. aureus* was added to HeLa cells showing vinculin knockdown and overexpressing GFP-Rab5 (WT), and the cell lysate was analyzed using a GST-R5BD pull-down assay. In contrast to the control cells, introduction of vinculin siRNA decreased the level of Rab5-GTP with the addition of *S. aureus* (Fig. 4C). These findings suggest that vinculin is involved in Rab5 activity in *S. aureus* uptake.

## Effect of active vinculin mutants on *S. aureus* uptake

We then investigated whether vinculin activation is involved in *S. aureus* uptake. Vinculin 8/19 (vin8/19) and vinculin T12 (vinT12) (Fig. 5A) interfere with the head-tail interaction characterizing constitutive activation [51]. Immunoprecipitation assays showed that GFP-vin8/19 and T12 strongly bound to Rab5 (Fig. 5B). Confocal fluorescence microscopic analysis revealed that GFP-vin8/19, GFP-vinT12 mutants and GFP-vin (WT) change the localization of HA-Rab5 and that the vinculin mutants and vin (WT) were colocalized with HA-Rab5 (WT) close to the plasma membrane. (Fig. 5C). Moreover, vin8/19 and T12 mutants strongly facilitated *S. aureus* uptake in cells. (Fig. 5D). We further investigated the effect of active vinculin mutants on Rab5 activation in *S. aureus* uptake using GST-R5BD. *S. aureus* was added to Cos-7 cells showing over-expression of active vinculin mutants and HA-Rab5 (WT), and the cell lysate was analyzed using a GST-R5BD pull-down assay. Over-expression of active vinculin mutants increased the level of Rab5-GTP with the addition of *S. aureus* (Fig. 5E). These findings suggest that vinculin activation is important for *S. aureus* uptake.

## Effect of inactive vinculin mutants on *S. aureus* uptake

Vinculin A50I (vinA50I) mutant (Fig. 6A) inhibits the head/tail dissociation of vinculin characterizing constitutive inactivation [52]. Immunoprecipitation assays showed that GFP-vinA50I did not bind to HA-Rab5 (WT) (Fig. 6B). Confocal fluorescence microscopic analysis revealed that vinA50I did not colocalize with

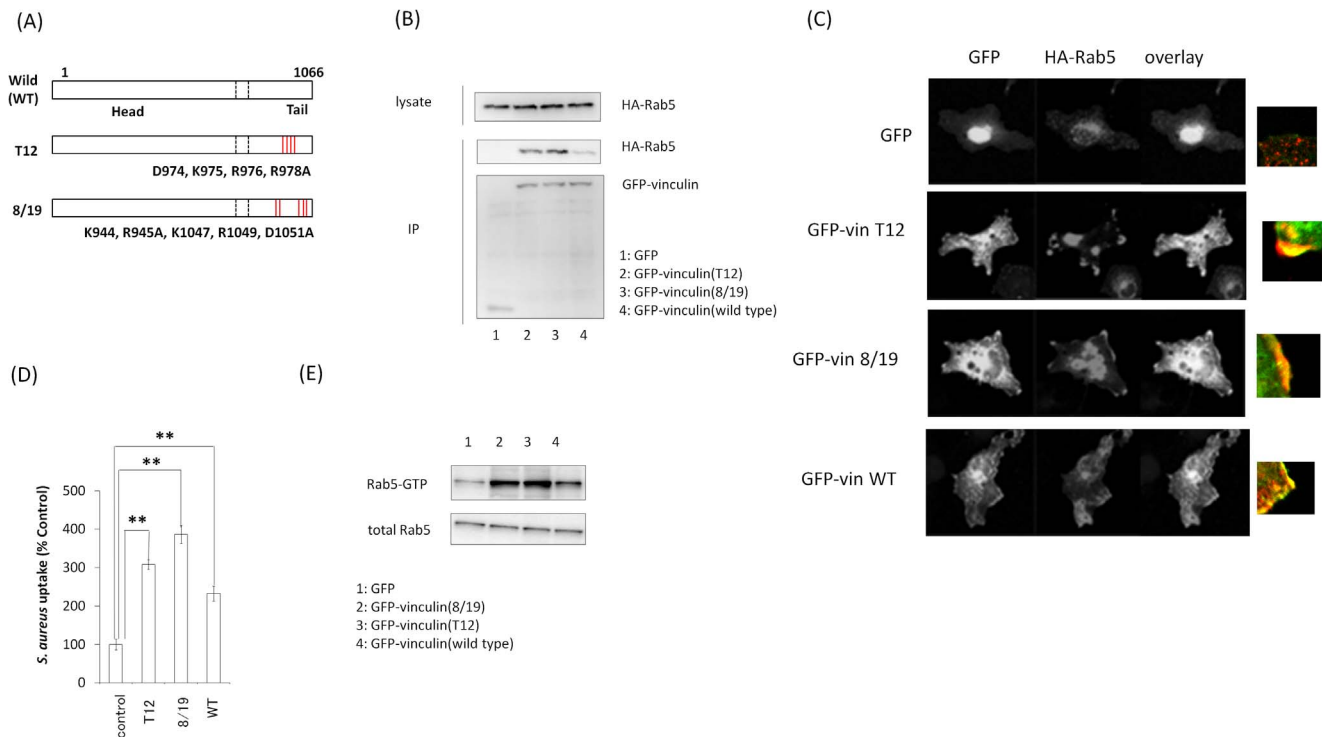


**Figure 5. Effect of vinculin-activated mutants on *S. aureus* uptake.** (A) Schematic of active vinculin mutants. (B) GFP, GFP-Vin8/19, GFP-VinT12, and GFP-vinculin (WT) were coexpressed with HA-Rab5 (WT) in Cos-7 cells, and these proteins were immunoprecipitated with anti-GFP antibody. Immunocomplexes were assayed by western blotting with anti-GFP and anti-HA antibodies. (C) GFP, GFP-Vin8/19, GFP-VinT12, and GFP-vinculin (WT) were coexpressed with HA-Rab5 (WT) in Cos-7 cells and immunostained with anti-HA antibody. (D) pHrodo red-labeled *S. aureus* was added to the medium of Cos-7 cells expressing active vinculin mutants and incubated for 2 h at 37°C. The graph shows mean  $\pm$  S.E. values of six independent experiments, \*\* $p < 0.01$ . (E) Cos-7 cells were transfected with HA-Rab5 (WT) and active vinculin mutants. *S. aureus* was added to the medium of transfected cells and incubated for 60 min at 37°C. The cells were lysed and subjected to a GST-R5BD pull-down assay. GST-R5BD-bound beads and lysates were assayed by western blotting with anti-HA antibody. doi:10.1371/journal.pone.0087373.g005

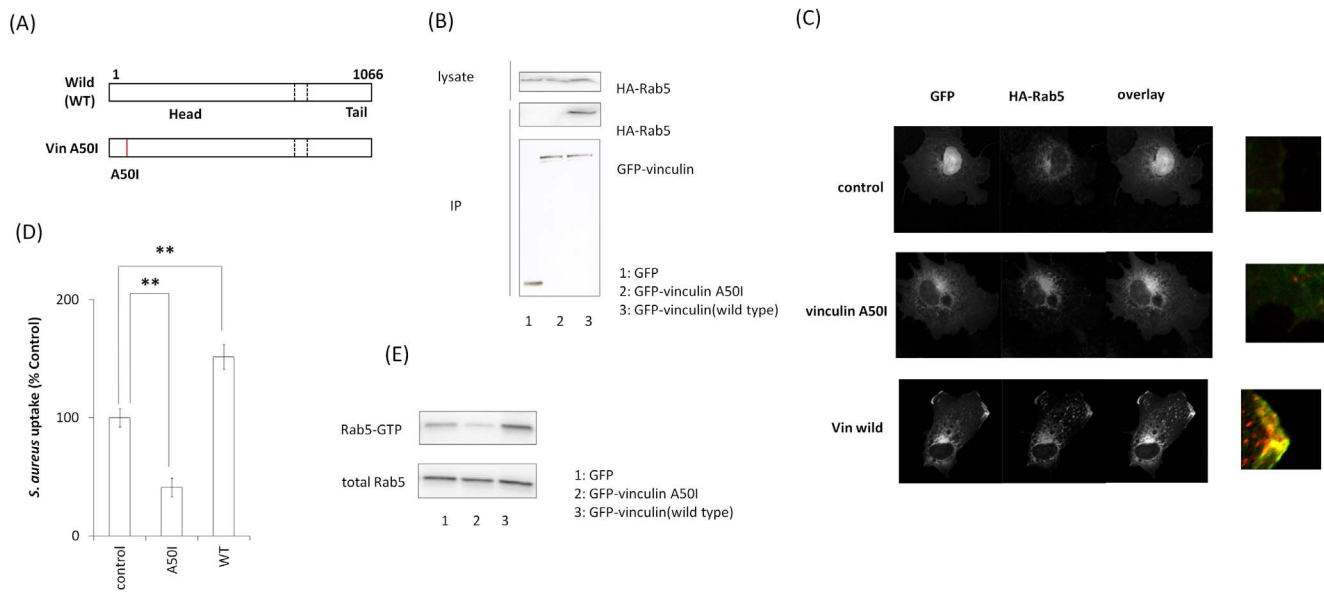


**Figure 6. Effect of vinculin-inactivated mutants on *S. aureus* uptake.** (A) Schematic of inactive vinculin mutants. (B) GFP, GFP-VinA50I, and GFP-vinculin (WT) were coexpressed with HA-Rab5 (WT) in Cos-7 cells, and these proteins were immunoprecipitated with anti-GFP antibody. Immunocomplexes were assayed by western blotting with anti-GFP and anti-HA antibodies. (C) GFP, GFP-VinA50I, and GFP-vinculin (WT) were coexpressed with HA-Rab5 (WT) in Cos-7 cells and immunostained with anti-HA antibody. (D) pHrodo red-labeled *S. aureus* was added to the medium of Cos-7 cells expressing inactive vinculin mutants and incubated for 2 h at 37°C. The graph shows mean  $\pm$  S.E. values of six independent experiments, \*\* $p < 0.01$ . (E) Cos-7 cells were transfected with HA-Rab5 (WT) and inactive vinculin mutants. *S. aureus* was added to the medium of transfected cells and incubated for 60 min at 37°C. The cells were lysed and subjected to a GST-R5BD pull-down assay. GST-R5BD-bound beads and lysates were assayed by western blotting with anti-HA antibody. doi:10.1371/journal.pone.0087373.g006

HA-Rab5 (WT) close to the plasma membrane (Fig. 6C). Moreover, vinA50I suppressed *S. aureus* uptake. (Fig. 6D). We further investigated the effect of the inactive vinculin mutant on Rab5 activation in *S. aureus* uptake using GST-R5BD. *S. aureus* was added to Cos-7 cells showing over-expression of the inactive vinculin mutant and HA-Rab5 (WT), and the cell lysate was analyzed using a GST-R5BD pull-down assay. Over-expression of the inactive vinculin mutant decreased the level of Rab5-GTP with the addition of *S. aureus* (Fig. 6E). These findings suggest that vinculin inactivation decreases *S. aureus* uptake.

### Functional analysis of the Rab5-binding domain of vinculin

Since vinculin directly bound to Rab5 (Fig. 1D), we next examined the Rab5-binding domain in vinculin. We constructed His-tagged deletion mutants of vinculin and examined the interaction with Rab5 by pull-down assays. As shown in Fig. 7A, His-vin1-258, His-vin1-880, and His-vin1-1066 (full length) bound to GST-Rab5 (Q79L), whereas vin258-880 and vin881-1066 did not (Fig. 7B). In addition, confocal fluorescence microscopic analysis showed that vin1-258, vin1-880, and vin1-1066 colocalized with HA-Rab5 (WT) close to the plasma membrane, but vin258-880 and vin881-1066 did not (Fig. 7C). These findings indicate that the N terminus of vinculin (vin1-258) can bind to Rab5. Next, we investigated the role of these vinculin mutants in *S. aureus* uptake. Cos-7 cells co-transfected with each of the vinculin mutants with HA-Rab5 were incubated with *S. aureus*. As shown in Fig. 7D, vin1-258, vin1-880, and vin1-1066 facilitated *S. aureus* uptake. Furthermore, Rab5-GTP induced by *S. aureus* was enhanced by over-expression of the vin1-258, vin1-880, and vin1-1066 in cos-7 cells (Fig. 7E). These findings suggest that N

terminus of vinculin (vin1-258) is important for vinculin-Rab5 binding and *S. aureus* uptake.

### Decrease in *S. aureus*-induced phosphorylation of p38, Erk and JNK and decrease in IL-6 expression by vinculin and Rab5 knockdown

MAPK is stimulated by bacterial infection, leading to cytokine expression [73]. We accordingly investigated whether *S. aureus* affects IL-6 expression via MAPK. p38, Erk, and JNK phosphorylation was increased by *S. aureus*. With vinculin and Rab5 knockdown, *S. aureus*-induced p38, Erk, and JNK phosphorylation in the cells was decreased (Fig. 8A and B). With vinculin and Rab5 knockdown, *S. aureus*-induced IL-6 expression was decreased in the cell lysate and medium (Fig. 8C and D). These results suggest that vinculin and Rab5 are involved in *S. aureus*-induced phosphorylation of p38, Erk and JNK and *S. aureus*-induced IL-6 expression.

### Functional consequences of vinculin and Rab5 knockdown *in vivo*

To obtain evidence for the importance of vinculin and Rab5 *in vivo*, we introduced siRNA into the mouse lung. First, we confirmed the knockdown levels of vinculin and Rab5 in the mouse lung after introducing siRNAs for vinculin and Rab5. Western blotting showed that the expression levels of vinculin and Rab5 in the lung were reduced by these siRNAs (Fig. 9A and B). We next infected mouse lungs with *S. aureus* and analyzed lung tissue by colony formation assays. In contrast to the control, vinculin knockdown reduced infection by *S. aureus* in mouse lungs (Fig. 9C). When Rab5 was knocked down, infection by *S. aureus* was also reduced in mouse lungs (Fig. 9D). Furthermore, *S. aureus*-



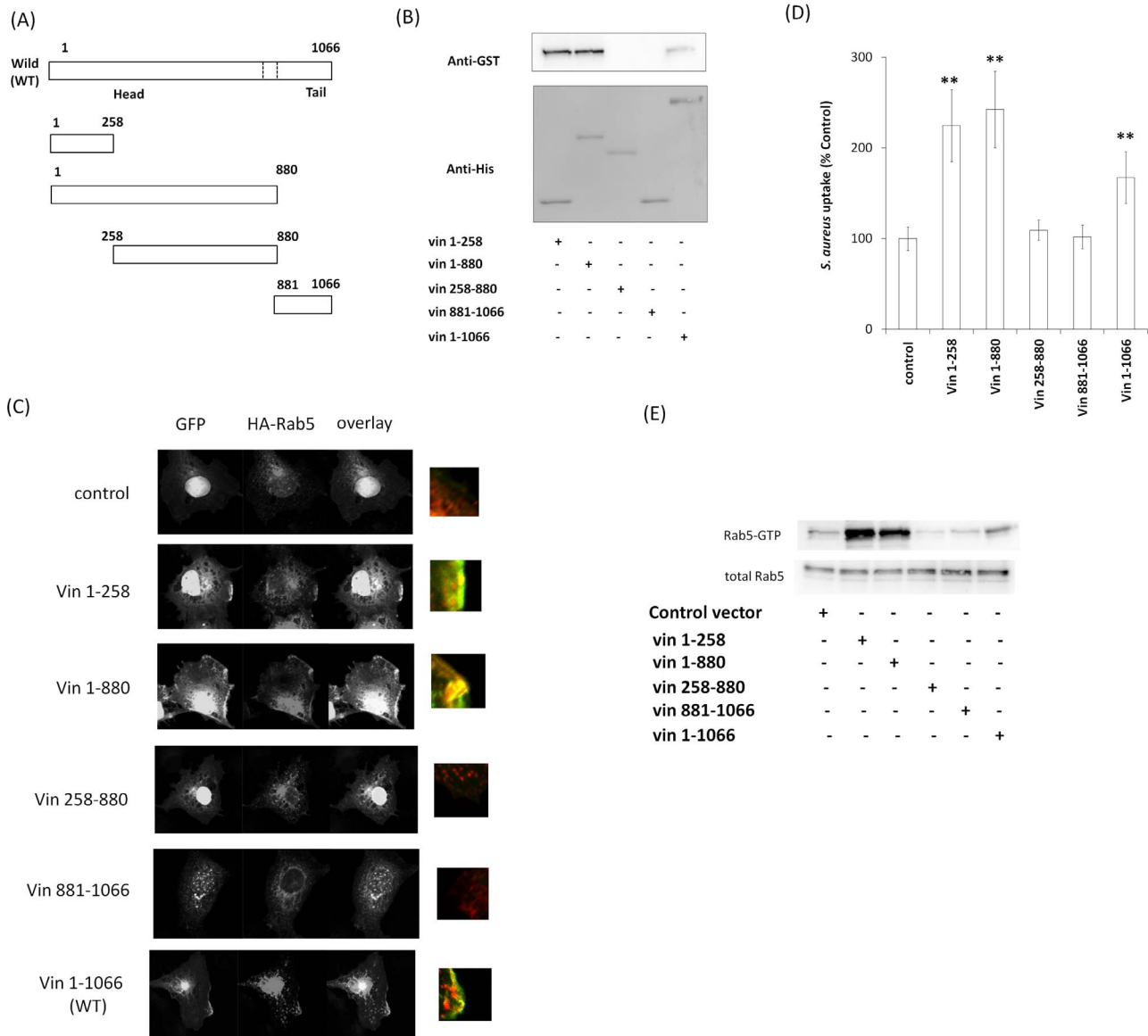


**Figure 7. Determination of the Rab5-binding domain of vinculin.** (A) Schematic of vinculin deletion mutants. (B) GST-Rab5 (Q79L) was incubated with purified His-vinculin deletion mutants, and a His-pull-down assay was performed. The beads were assayed by western blotting. (C) GFP, GFP-Vin1-258, GFP-Vin1-880, GFP-Vin258-880, GFP-Vin881-1066 and GFP-vinculin (full length) were coexpressed with HA-Rab5 in Cos-7 cells and immunostained with anti-HA antibody. (D) pHrodo red-labeled *S. aureus* was added to the medium of Cos-7 cells expressing each vinculin deletion mutant and incubated for 2 h at 37°C. The graph shows mean ± S.E. values of six independent experiments, \*\**p*<0.01. (E) Cos-7 cells were transfected with HA-Rab5 (WT) and vinculin deletion mutants. *S. aureus* was added to the medium of transfected cells and incubated for 60 min at 37°C. The cells were lysed and subjected to a GST-R5BD pull-down assay. GST-R5BD-bound beads and lysates were assayed by western blotting with anti-HA antibody. doi:10.1371/journal.pone.0087373.g007

induced p38, Erk, and JNK phosphorylation in the mouse lung decreased with vinculin and Rab5 knockdown (Fig. 9E and F). Moreover, *S. aureus*-induced IL-6 expression in the mouse lung decreased with vinculin and Rab5 knockdown (Fig. 9G and H).

**Discussion**

In this study, we demonstrated that vinculin interacts with Rab5 and modulates functions of the protein in manner different from those for other well-known Rab5-interacting proteins as follows. First, vinculin is a focal adhesion protein, unlike other Rab5-interacting proteins (Rabaptin-5, EEA1, and Rabex-5), which are

recruited to early endosome membranes by active Rab5 [2,20,74]. Second, vinculin interacts with both inactive Rab5 and active Rab5, and this property also distinct from EEA-1, Rabex-5, and Rabaptin-5. Third, vinculin appears to participate in only phagocytosis (internalization of *S. aureus* into cells).

Recent findings suggest that vinculin may participate in the phagocytosis of collagen beads [55]. In the present study, vinculin was shown to be involved in *S. aureus* uptake but not in the uptakes of transferrin, albumin, Lucifer yellow, or FM4-64 (Fig. 2A–E and Fig. 3B–F). Phagocytosis is a process by which cells engulf large particles, usually over 0.5 μm in diameter [75]. *S. aureus* is over 0.5 μm in diameter, and cells engulf *S. aureus* by phagocytosis via

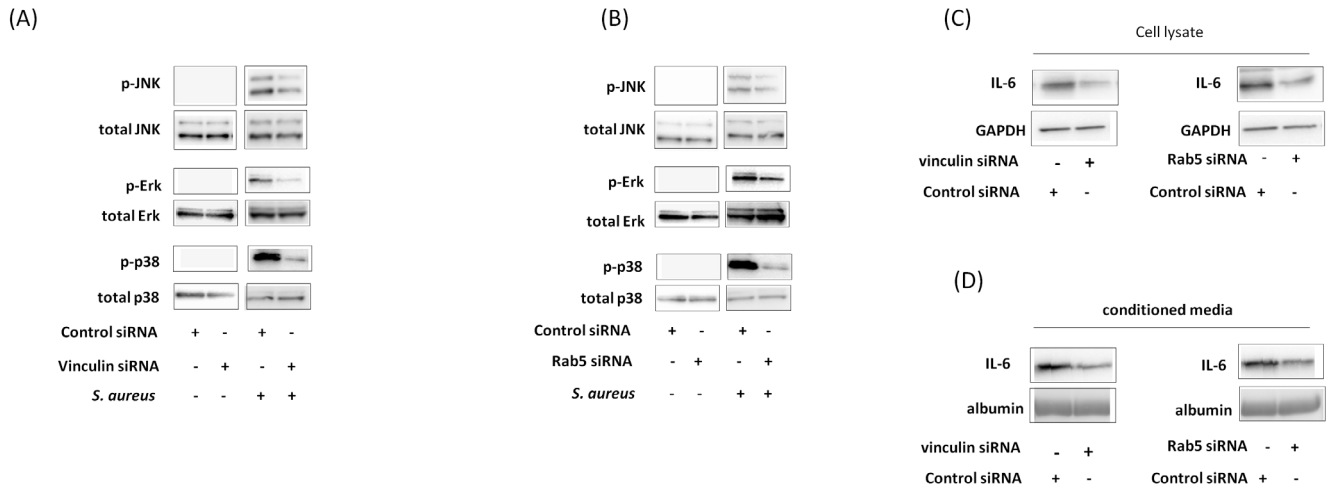


**Figure 8. Effect of vinculin and Rab5 knockdown on *S. aureus*-induced IL-6 expression.** (A and B) *S. aureus* was added to the medium of HeLa cells with vinculin (A) or Rab5 (B) knockdown and incubated for 60 min at 37°C. The cell lysates were assayed with anti-JNK, anti-phosphor-JNK, anti-ERK, anti-phosphor-Erk, anti-p38, and anti-phosphor-p38 antibodies by western blotting. (C and D) *S. aureus* was added to the medium of HeLa cells with vinculin or Rab5 knockdown and incubated for 16 h. The cell lysate (C) and conditioned medium (D) were assayed with anti-IL-6 antibody by western blotting. GAPDH and albumin were internal controls. doi:10.1371/journal.pone.0087373.g008

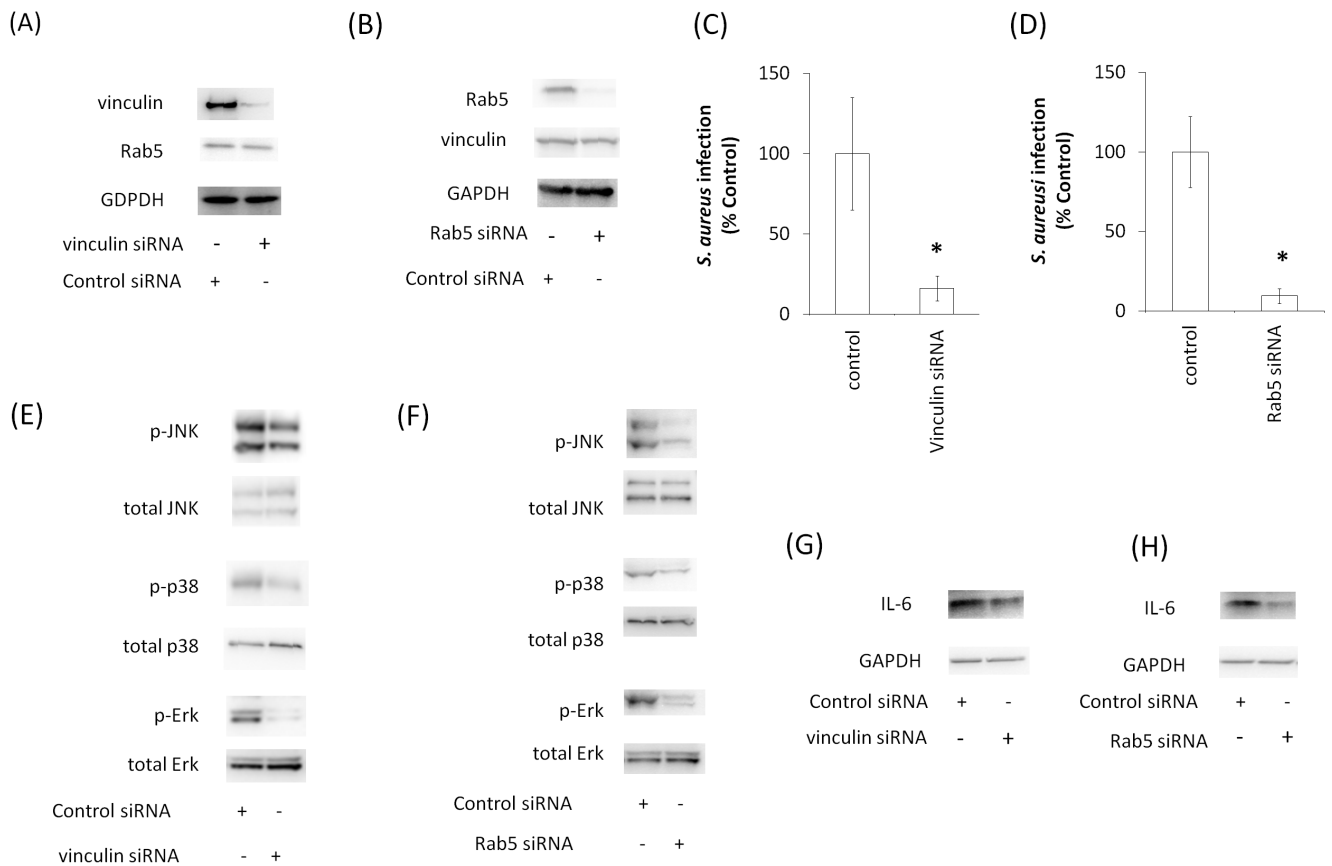


**Figure 9. Effects of vinculin and Rab5 knockdown on *S. aureus* infection in murine lung.** (A and B) Mouse lungs were transfected with vinculin and Rab5 siRNA. After 3 days, lungs were homogenized and treated with anti-vinculin, anti-Rab5, and anti-GAPDH (internal control) antibodies. (C and D) Murine lungs in which vinculin or Rab5 had been knocked down were infected with *S. aureus*. Lung tissues were analyzed for colony formation. The graph shows the mean  $\pm$  S.E. of five independent experiments. (E–F) Murine lung in which vinculin (E and G) or Rab5 (F and H) had been knocked down was infected with *S. aureus*. The murine lung homogenates were assayed with anti-JNK, anti-phosphor-JNK, anti-ERK, anti-phosphor-Erk, anti-p38, anti-phosphor-p38, anti-IL-6, and anti-GAPDH (internal control) antibodies by western blotting. doi:10.1371/journal.pone.0087373.g009

cell surface receptor such as integrins [76]. In contrast, the sizes of transferrin, albumin, Lucifer yellow and FM4-64 are very small and thus they do not induce phagocytosis. Transferrin is internalized to cells by clathrin-dependent endocytosis via the transferrin receptor [77]. Albumin is mainly incorporated into cells by caveolae-dependent endocytosis via gp60, an albumin receptor [78]. Lucifer yellow and FM4-64, which do not have specific receptors, are ingested by fluid-phase endocytosis [79,80,81]. It is likely that vinculin cannot participate in receptor-mediated endocytosis of small molecules and fluid-phase endocytosis; however, vinculin may be a critical protein for endocytosis of large molecules such as those incorporated into cells by phagocytosis.

In the present study, vinculin was shown to bind to both inactive and active Rab5 (Fig. 1B–D) and to be involved in Rab5 activation during *S. aureus* uptake (Fig. 4C). Rab5 activation requires interaction with GEF, which contains a specific, highly conserved domain (Vps9) that catalyzes nucleotide exchange on Rab5 [20,82,83,84,85,86,87,88,89]. However, the amino acid sequence of vinculin does not contain a Vps9 domain. RabGDIs regulates the GDP/GTP exchange reaction of most Rab proteins by inhibiting the dissociation of GDP from them and the subsequent binding of GTP to them [4]. Although we have not uncovered the mechanism of vinculin-mediated Rab5 activation, vinculin may release RabGDI from Rab5-GDP or associate with GEF. Moreover, our data indicated that vinculin could bind more strongly to active Rab5 than to inactive Rab5, although vinculin bound to both of the molecules (Fig. 1B–D). Active Rab5 is crucial for vesicle transportation in the early stage of endocytosis (also phagocytosis) and early endosome fusion [2,4]. It is possible that vinculin is involved in vesicle transport and/or endosome fusion in the early stage of phagocytosis. In support of this, we have observed that there are interactions between vinculin and other early endosome proteins such as EEA1 and Rabaptin-5 (our unpublished data).

Assays with active vinculin mutants (vinT12 and vin8/19) showed that vinculin activation facilitated vinculin–Rab5 binding and *S. aureus* uptake (Fig. 5B and D), whereas an inactive vinculin mutant (vinA50I) decreased *S. aureus* uptake (Fig. 6D). It was recently shown that active vinculin mutants recruit vinxin, a vinculin-interacting protein, to the plasma membrane [48]. It is

possible that active vinculin also recruits Rab5 to the plasma membrane, thereby inducing phagocytosis of *S. aureus*.

*S. aureus*, a gram-positive pathogen, has long been recognized as one of the most important bacteria that cause various diseases including pneumonia [90]. *In vitro* studies have shown that *S. aureus* is internalized and survives inside non-phagocytic cells [62]. Internalized *S. aureus* is able to evade or delay elimination by the host's immune system and avoid extracellular antibiotics [66]. Therefore, a drug that inhibits internalization of *S. aureus* into non-phagocytic cells could be valuable for therapy of pneumonia. Our data showed that vinculin and Rab5 participated in infection of *S. aureus* in the mouse lung (Fig. 9C and D). Both vinculin and Rab5 knockdown also decreased *S. aureus*-induced IL-6 expression (Fig. 9E–H), indicating that inflammation was inhibited. Vinculin might be a target of therapy for various *S. aureus*-induced diseases including pneumonia.

In conclusion, we have shown that vinculin interacts directly with Rab5 and that its interaction is involved in *S. aureus* uptake. However, we did not observe uptake of other substances under the influence of vinculin–Rab5 interaction. Vinculin could interact with Rab5 without *S. aureus* (Fig. 1A–D). Vinculin underpins integrin under the plasma membrane, and integrin binds to extracellular matrix proteins, many bacteria, bacterial pathogens and viruses [91,92,93]. A recent study showed that R-Ras/Rin/Rab5 complex controls endothelial cell adhesion and morphogenesis via active integrin endocytosis [94]. To elucidate the precise molecular mechanisms, further studies are needed to provide new insights into the mechanisms of cellular uptake through vinculin–Rab5 interaction.

## Acknowledgments

The authors thank Susan W. Craig (Johns Hopkins University) for the vinT12 and vin8/19 constructs. The authors also thank Guangpu Li (University of Oklahoma) for the GST-R5BD construct, and Yuji Yamamoto (Tokyo University of Agriculture) for the Rab5 construct.

## Author Contributions

Conceived and designed the experiments: MH KM. Performed the experiments: MH EK. Analyzed the data: MH EK SS TK HT RI NT YK NI KK MN KI KM. Contributed reagents/materials/analysis tools: MH EK SS TK KI. Wrote the paper: MH KM.

## References

- Hutagalung AH, Novick PJ (2011) Role of Rab GTPases in membrane traffic and cell physiology. *Physiol Rev* 91: 119–149.
- Zerial M, McBride H (2001) Rab proteins as membrane organizers. *Nat Rev Mol Cell Biol* 2: 107–117.
- Brighouse A, Dacks JB, Field MC (2010) Rab protein evolution and the history of the eukaryotic endomembrane system. *Cell Mol Life Sci* 67: 3449–3465.
- Stenmark H (2009) Rab GTPases as coordinators of vesicle traffic. *Nat Rev Mol Cell Biol* 10: 513–525.
- Stenmark H, Olkkonen VM (2001) The Rab GTPase family. *Genome Biol* 2: REVIEWS3007.
- Huang SN, Phelps MA, Swaan PW (2003) Involvement of endocytic organelles in the subcellular trafficking and localization of riboflavin. *J Pharmacol Exp Ther* 306: 681–687.
- Leonard D, Hayakawa A, Lawe D, Lambright D, Bellve KD, et al. (2008) Sorting of EGF and transferrin at the plasma membrane and by cargo-specific signaling to EEA1-enriched endosomes. *J Cell Sci* 121: 3445–3458.
- Benmerah A (2004) Endocytosis: signaling from endocytic membranes to the nucleus. *Curr Biol* 14: R314–316.
- Lanzetti L, Rybin V, Malabarba MG, Christoforidis S, Scita G, et al. (2000) The Eps8 protein coordinates EGF receptor signalling through Rac and trafficking through Rab5. *Nature* 408: 374–377.
- Macovei A, Petrareanu C, Lazar C, Florian P, Branza-Nichita N (2013) Regulation of hepatitis B virus infection by Rab5, Rab7, and the endolysosomal compartment. *J Virol* 87: 6415–6427.
- Kalia M, Khasa R, Sharma M, Nain M, Vratil S (2013) Japanese encephalitis virus infects neuronal cells through a clathrin-independent endocytic mechanism. *J Virol* 87: 148–162.
- Acosta EG, Castilla V, Damonte EB (2012) Differential requirements in endocytic trafficking for penetration of dengue virus. *PLoS One* 7: e44835.
- Hollinshead M, Johns HL, Sayers CL, Gonzalez-Lopez C, Smith GL, et al. (2012) Endocytic tubules regulated by Rab GTPases 5 and 11 are used for envelopment of herpes simplex virus. *EMBO J* 31: 4204–4220.
- Lee JJ, Kim DG, Kim DH, Simborio HL, Min W, et al. (2013) Interplay between Clathrin and Rab5 Controls the Early Phagocytic Trafficking and Intracellular Survival of *Brucella abortus* within HeLa cells. *J Biol Chem* 288: 28049–28057.
- Newton HJ, McDonough JA, Roy CR (2013) Effector protein translocation by the *Coxiella burnetii* Dot/Icm type IV secretion system requires endocytic maturation of the pathogen-occupied vacuole. *PLoS One* 8: e54566.
- Bhattacharya M, Ojha N, Solanki S, Mukhopadhyay CK, Madan R, et al. (2006) IL-6 and IL-12 specifically regulate the expression of Rab5 and Rab7 via distinct signaling pathways. *EMBO J* 25: 2878–2888.
- Mustafi S, Rivero N, Olson JC, Stahl PD, Barbieri MA (2013) Regulation of Rab5 function during phagocytosis of live *Pseudomonas aeruginosa* in macrophages. *Infect Immun* 81: 2426–2436.
- Christoforidis S, McBride HM, Burgoyne RD, Zerial M (1999) The Rab5 effector EEA1 is a core component of endosome docking. *Nature* 397: 621–625.
- Merithew E, Stone C, Eathiraj S, Lambright DG (2003) Determinants of Rab5 interaction with the N terminus of early endosome antigen 1. *J Biol Chem* 278: 8494–8500.

20. Horiuchi H, Lippe R, McBride HM, Rubino M, Woodman P, et al. (1997) A novel Rab5 GDP/GTP exchange factor complexed to Rabaptin-5 links nucleotide exchange to effector recruitment and function. *Cell* 90: 1149–1159.
21. Thomas C, Strutt D (2013) Rabaptin-5 and Rabex-5 are neoplastic tumour suppressor genes that interact to modulate Rab5 dynamics in *Drosophila melanogaster*. *Dev Biol*.
22. Zhu H, Qian H, Li G (2010) Delayed onset of positive feedback activation of Rab5 by Rabex-5 and Rabaptin-5 in endocytosis. *PLoS One* 5: e9226.
23. Simonsen A, Lippe R, Christoforidis S, Gaullier JM, Brech A, et al. (1998) EEA1 links PI(3)K function to Rab5 regulation of endosome fusion. *Nature* 394: 494–498.
24. Chamberlain MD, Chan T, Oberg JC, Hawrysh AD, James KM, et al. (2008) Disrupted RabGAP function of the p85 subunit of phosphatidylinositol 3-kinase results in cell transformation. *J Biol Chem* 283: 15861–15868.
25. Fabrowski P, Necakov AS, Mumbauer S, Loeser E, Reversi A, et al. (2013) Tubular endocytosis drives remodelling of the apical surface during epithelial morphogenesis in *Drosophila*. *Nat Commun* 4: 2244.
26. Schnatwinkel C, Christoforidis S, Lindsay MR, Uttenweiler-Joseph S, Wilm M, et al. (2004) The Rab5 effector Rabankyrin-5 regulates and coordinates different endocytic mechanisms. *PLoS Biol* 2: E261.
27. Epp N, Ungermann C (2013) The N-terminal domains of Vps3 and Vps8 are critical for localization and function of the CORVET tethering complex on endosomes. *PLoS One* 8: e67307.
28. Hagiwara M, Komatsu T, Sugiura SS, Isoda R, Tada H, et al. (2013) POT1b regulates phagocytosis and NO production by modulating activity of the small GTPase Rab5. *Biochem Biophys Res Commun* 439: 413–417.
29. Hagiwara M, Shirai Y, Nomura R, Sasaki M, Kobayashi K, et al. (2009) Caveolin-1 activates Rab5 and enhances endocytosis through direct interaction. *Biochem Biophys Res Commun* 378: 73–78.
30. Pelkmans L, Burli T, Zerial M, Helenius A (2004) Caveolin-stabilized membrane domains as multifunctional transport and sorting devices in endocytic membrane traffic. *Cell* 118: 767–780.
31. Hagiwara M, Shinomiya H, Kashihara M, Kobayashi K, Tadokoro T, et al. (2011) Interaction of activated Rab5 with actin-bundling proteins, L- and T-plastin and its relevance to endocytic functions in mammalian cells. *Biochem Biophys Res Commun* 407: 615–619.
32. Ziegler WH, Liddington RC, Critchley DR (2006) The structure and regulation of vinculin. *Trends Cell Biol* 16: 453–460.
33. Izard T, Vornheim C (2004) Structural basis for amplifying vinculin activation by talin. *J Biol Chem* 279: 27667–27678.
34. Izard T, Evans G, Borgon RA, Rush CL, Bricogne G, et al. (2004) Vinculin activation by talin through helical bundle conversion. *Nature* 427: 171–175.
35. Humphries JD, Wang P, Streuli C, Geiger B, Humphries MJ, et al. (2007) Vinculin controls focal adhesion formation by direct interactions with talin and actin. *J Cell Biol* 179: 1043–1057.
36. Bois PR, O'Hara BP, Nietispach D, Kirkpatrick J, Izard T (2006) The vinculin binding sites of talin and alpha-actinin are sufficient to activate vinculin. *J Biol Chem* 281: 7228–7236.
37. Menkel AR, Kroemker M, Bubeck P, Ronsiek M, Nikolai G, et al. (1994) Characterization of an F-actin-binding domain in the cytoskeletal protein vinculin. *J Cell Biol* 126: 1231–1240.
38. Shen K, Tolbert CE, Gullity C, Swaminathan VS, Berginski ME, et al. (2011) The vinculin C-terminal hairpin mediates F-actin bundle formation, focal adhesion, and cell mechanical properties. *J Biol Chem* 286: 45103–45115.
39. DeMali KA, Barlow CA, Burridge K (2002) Recruitment of the Arp2/3 complex to vinculin: coupling membrane protrusion to matrix adhesion. *J Cell Biol* 159: 881–891.
40. Rangarajan ES, Izard T (2012) The cytoskeletal protein alpha-catenin unfurls upon binding to vinculin. *J Biol Chem* 287: 18492–18499.
41. Peng X, Maier JL, Choudhury D, Craig SW, DeMali KA (2012) alpha-Catenin uses a novel mechanism to activate vinculin. *J Biol Chem* 287: 7728–7737.
42. Ishiyama N, Tanaka N, Abe K, Yang YJ, Abbas YM, et al. (2013) An autoinhibited structure of alpha-catenin and its implications for vinculin recruitment to adherens junctions. *J Biol Chem* 288: 15913–15925.
43. Thomas WA, Boscher C, Chu YS, Cuvelier D, Martinez-Rico C, et al. (2013) alpha-Catenin and vinculin cooperate to promote high E-cadherin-based adhesion strength. *J Biol Chem* 288: 4957–4969.
44. Deakin NO, Ballestrem C, Turner CE (2012) Paxillin and Hic-5 interaction with vinculin is differentially regulated by Rac1 and RhoA. *PLoS One* 7: e37990.
45. Brindle NP, Holt MR, Davies JE, Price CJ, Critchley DR (1996) The focal-adhesion vasodilator-stimulated phosphoprotein (VASP) binds to the proline-rich domain in vinculin. *Biochem J* 318 (Pt 3): 753–757.
46. Kioka N, Sakata S, Kawachi T, Amachi T, Akiyama SK, et al. (1999) Vinexin: a novel vinculin-binding protein with multiple SH3 domains enhances actin cytoskeletal organization. *J Cell Biol* 144: 59–69.
47. Umemoto T, Tanaka K, Ueda K, Kioka N (2009) Tyrosine phosphorylation of vinexin in v-Src-transformed cells attenuates the affinity for vinculin. *Biochem Biophys Res Commun* 387: 191–195.
48. Takahashi H, Mitsushima M, Okada N, Ito T, Aizawa S, et al. (2005) Role of interaction with vinculin in recruitment of vinexins to focal adhesions. *Biochem Biophys Res Commun* 336: 239–246.
49. Zamir E, Geiger B (2001) Molecular complexity and dynamics of cell-matrix adhesions. *J Cell Sci* 114: 3583–3590.
50. Bakolitsa C, Cohen DM, Bankston LA, Bobkov AA, Cadwell GW, et al. (2004) Structural basis for vinculin activation at sites of cell adhesion. *Nature* 430: 583–586.
51. Cohen DM, Chen H, Johnson RP, Choudhury B, Craig SW (2005) Two distinct head-tail interfaces cooperate to suppress activation of vinculin by talin. *J Biol Chem* 280: 17109–17117.
52. Diez G, Auernheimer V, Fabry B, Goldmann WH (2011) Head/tail interaction of vinculin influences cell mechanical behavior. *Biochem Biophys Res Commun* 406: 85–88.
53. Cohen DM, Kutscher B, Chen H, Murphy DB, Craig SW (2006) A conformational switch in vinculin drives formation and dynamics of a talin-vinculin complex at focal adhesions. *J Biol Chem* 281: 16006–16015.
54. Chandrasekar I, Stradal TE, Holt MR, Entschladen F, Jockusch BM, et al. (2005) Vinculin acts as a sensor in lipid regulation of adhesion-site turnover. *J Cell Sci* 118: 1461–1472.
55. Arora PD, Conti MA, Ravid S, Sacks DB, Kapus A, et al. (2008) Rap1 activation in collagen phagocytosis is dependent on nonmuscle myosin II-A. *Mol Biol Cell* 19: 5032–5046.
56. Raman M, Chen W, Cobb MH (2007) Differential regulation and properties of MAPKs. *Oncogene* 26: 3100–3112.
57. Qi M, Elion EA (2005) MAP kinase pathways. *J Cell Sci* 118: 3569–3572.
58. Hu CT, Wu JR, Wu WS (2013) The role of endosomal signaling triggered by metastatic growth factors in tumor progression. *Cell Signal* 25: 1539–1545.
59. Liu W, Tundwal K, Liang Q, Goplen N, Rozario S, et al. (2010) Establishment of extracellular signal-regulated kinase 1/2 bistability and sustained activation through Sprouty 2 and its relevance for epithelial function. *Mol Cell Biol* 30: 1783–1799.
60. Law IK, Murphy JE, Bakirtzi K, Bunnett NW, Pothoulakis C (2012) Neurotensin-induced proinflammatory signaling in human colonocytes is regulated by beta-arrestins and endothelin-converting enzyme-1-dependent endocytosis and resensitization of neurotensin receptor 1. *J Biol Chem* 287: 15066–15075.
61. Chen XQ, Wang B, Wu C, Pan J, Yuan B, et al. (2012) Endosome-mediated retrograde axonal transport of P2X3 receptor signals in primary sensory neurons. *Cell Res* 22: 677–696.
62. Hoffmann C, Ohlsen K, Hauck CR (2011) Integrin-mediated uptake of fibronectin-binding bacteria. *Eur J Cell Biol* 90: 891–896.
63. Ahmed S, Meghji S, Williams RJ, Henderson B, Brock JH, et al. (2001) Staphylococcus aureus fibronectin binding proteins are essential for internalization by osteoblasts but do not account for differences in intracellular levels of bacteria. *Infect Immun* 69: 2872–2877.
64. Almeida RA, Matthews KR, Cifrian E, Guidry AJ, Oliver SP (1996) Staphylococcus aureus invasion of bovine mammary epithelial cells. *J Dairy Sci* 79: 1021–1026.
65. Grosz M, Kolter J, Paprotka K, Winkler AC, Schafer D, et al. (2013) Cytoplasmic replication of Staphylococcus aureus upon phagosomal escape triggered by phenol-soluble modulins alpha. *Cell Microbiol*.
66. Lowy FD (2000) Is Staphylococcus aureus an intracellular pathogen? *Trends Microbiol* 8: 341–343.
67. Liu J, Lamb D, Chou MM, Liu YJ, Li G (2007) Nerve growth factor-mediated neurite outgrowth via regulation of Rab5. *Mol Biol Cell* 18: 1375–1384.
68. Hagiwara M, Kobayashi K, Tadokoro T, Yamamoto Y (2010) Application of SYPRO Ruby- and Flamingo-stained polyacrylamide gels to Western blot analysis. *Anal Biochem* 397: 262–264.
69. Hagiwara M, Kobayashi K, Tadokoro T, Yamamoto Y (2009) Rab5 affinity chromatography without nonhydrolyzable GTP analogues. *Z Naturforsch C* 64: 303–306.
70. Leclerc EA, Gazeilles L, Serre G, Guerrin M, Jonca N (2011) The ubiquitous demokine delta activates Rab5 function in the early endocytic pathway. *PLoS One* 6: e17816.
71. Zwaenepoel O, Tzenaki N, Vergetaki A, Makrigiannakis A, Vanhaesebroeck B, et al. (2012) Functional CSF-1 receptors are located at the nuclear envelope and activated via the p110delta isoform of PI 3-kinase. *FASEB J* 26: 691–706.
72. Kimizuka R, Kato T, Ishihara K, Okuda K (2003) Mixed infections with Porphyromonas gingivalis and Treponema denticola cause excessive inflammatory responses in a mouse pneumonia model compared with monoinfections. *Microbes Infect* 5: 1357–1362.
73. Krachler AM, Woolery AR, Orth K (2011) Manipulation of kinase signaling by bacterial pathogens. *J Cell Biol* 195: 1083–1092.
74. Stenmark H, Vitale G, Ullrich O, Zerial M (1995) Rabaptin-5 is a direct effector of the small GTPase Rab5 in endocytic membrane fusion. *Cell* 83: 423–432.
75. Garcia-Garcia E, Rosales C (2002) Signal transduction during Fc receptor-mediated phagocytosis. *J Leukoc Biol* 72: 1092–1108.
76. Sinha B, Francois PP, Nusse O, Foti M, Hartford OM, et al. (1999) Fibronectin-binding protein acts as Staphylococcus aureus invasin via fibronectin bridging to integrin alpha5beta1. *Cell Microbiol* 1: 101–117.
77. Le Roy C, Wrana JL (2005) Clathrin- and non-clathrin-mediated endocytic regulation of cell signalling. *Nat Rev Mol Cell Biol* 6: 112–126.
78. John TA, Vogel SM, Tirupathi C, Malik AB, Minshall RD (2003) Quantitative analysis of albumin uptake and transport in the rat microvessel endothelial monolayer. *Am J Physiol Lung Cell Mol Physiol* 284: L187–196.
79. Wiederkehr A, Meier KD, Riezman H (2001) Identification and characterization of Saccharomyces cerevisiae mutants defective in fluid-phase endocytosis. *Yeast* 18: 759–773.

80. Johnson C, Kannan TR, Baseman JB (2011) Cellular vacuoles induced by *Mycoplasma pneumoniae* CARDS toxin originate from Rab9-associated compartments. *PLoS One* 6: e22877.
81. Tuo S, Nakashima K, Pringle JR (2013) Role of endocytosis in localization and maintenance of the spatial markers for bud-site selection in yeast. *PLoS One* 8: e72123.
82. Carney DS, Davies BA, Horazdovsky BF (2006) Vps9 domain-containing proteins: activators of Rab5 GTPases from yeast to neurons. *Trends Cell Biol* 16: 27–35.
83. Tall GG, Barbieri MA, Stahl PD, Horazdovsky BF (2001) Ras-activated endocytosis is mediated by the Rab5 guanine nucleotide exchange activity of RIN1. *Dev Cell* 1: 73–82.
84. Woller B, Luiskandl S, Popovic M, Prieler BE, Ikonge G, et al. (2011) Rin-like, a novel regulator of endocytosis, acts as guanine nucleotide exchange factor for Rab5a and Rab22. *Biochim Biophys Acta* 1813: 1198–1210.
85. Kajihō H, Fukushima S, Kontani K, Katada T (2012) RINL, guanine nucleotide exchange factor Rab5-subfamily, is involved in the EphA8-degradation pathway with odin. *PLoS One* 7: e30575.
86. Topp JD, Gray NW, Gerard RD, Horazdovsky BF (2004) Alsln is a Rab5 and Rac1 guanine nucleotide exchange factor. *J Biol Chem* 279: 24612–24623.
87. Kajihō H, Saito K, Tsujita K, Kontani K, Araki Y, et al. (2003) RIN3: a novel Rab5 GEF interacting with amphiphysin II involved in the early endocytic pathway. *J Cell Sci* 116: 4159–4168.
88. Saito K, Murai J, Kajihō H, Kontani K, Kurosu H, et al. (2002) A novel binding protein composed of homophilic tetramer exhibits unique properties for the small GTPase Rab5. *J Biol Chem* 277: 3412–3418.
89. Paulsel AL, Merz AJ, Nickerson DP (2013) Vps9 family protein Muk1 is the second Rab5 guanosine nucleotide exchange factor in budding yeast. *J Biol Chem* 288: 18162–18171.
90. Polyzos KA, Mavros MN, Vardakas KZ, Makris MC, Rafailidis PI, et al. (2012) Efficacy and safety of telavancin in clinical trials: a systematic review and meta-analysis. *PLoS One* 7: e41870.
91. Dupuy AG, Caron E (2008) Integrin-dependent phagocytosis: spreading from microadhesion to new concepts. *J Cell Sci* 121: 1773–1783.
92. Campadelli-Fiume G, Menotti L, Avitabile E, Gianni T (2012) Viral and cellular contributions to herpes simplex virus entry into the cell. *Curr Opin Virol* 2: 28–36.
93. Hauck CR, Borisova M, Muenzner P (2012) Exploitation of integrin function by pathogenic microbes. *Curr Opin Cell Biol* 24: 637–644.
94. Sandri C, Caccavari F, Valdembri D, Camillo C, Veltel S, et al. (2012) The R-Ras/RIN2/Rab5 complex controls endothelial cell adhesion and morphogenesis via active integrin endocytosis and Rac signaling. *Cell Res* 22: 1479–1501.